Collisional effects in Stark spectroscopy of molecules in 1Π electronic states

Millard H. Alexander

Citation: The Journal of Chemical Physics **83**, 3340 (1985); doi: 10.1063/1.449195
View online: http://dx.doi.org/10.1063/1.449195
View Table of Contents: http://scitation.aip.org/content/aip/journal/jcp/83/7?ver=pdfcov
Published by the AIP Publishing

Collisional effects in Stark spectroscopy of molecules in $^1\Pi$ electronic states

Millard H. Alexander
Department of Chemistry, University of Maryland, College Park, Maryland 20742

(Received 21 January 1985; accepted 18 June 1985)

We present the theoretical framework necessary to describe inelastic collisions between Stark mixed Λ-doublet levels of a molecule in a $^1\Pi$ electronic state, and the subsequent effect on fluorescence intensities. It is convenient to work with the spherical tensor moments of the excited state density matrix. For weak fields and short times after excitation the ratio of the fluorescence intensities for emission on "forbidden" and allowed $^1\Sigma^+ \leftarrow {}^1\Pi$ lines is predicted to vary linearly with time and quadratically with field strength. Simulation studies are presented, based on collisional parameters suggested by previous theoretical studies of inelastic collisions of molecules in Π electronic states. The present article provides the foundation for the accurate interpretation of laser diagnostic studies in plasma environments, such as those described by Mandich, Gaebe, and Gottscho in the accompanying article.

I. INTRODUCTION

Recently, Moore, Davis, and Gottscho[1] have introduced a novel technique for *in situ* measurement of plasma electric field strengths. The idea is as follows: A pulsed dye laser is used to excite an individual Λ-doublet level in an excited electronic state of $^1\Pi$ symmetry. In the absence of an electric field the two Λ-doublet levels correspond to electronic wave functions of opposite symmetry with respect to inversion in the plane of the molecule.[2] These two wave functions are mixed by the field, so that "symmetry forbidden" lines appear in the fluorescence spectrum of the excited molecule.[3] A comparison of the intensity of these forbidden lines to the intensity of the "symmetry allowed" lines is a sensitive function of the local electric field. Gottscho *et al.*[1] realized that this laser diagnostic technique provides, in principle, a means to obtain highly resolved information about the spatial and temporal distributions of electric fields in plasmas, which is of considerable importance in microelectronic plasma processing.[4] A more detailed description of this new laser induced fluorescence technique is given in the accompanying article by Mandich, Gaebe, and Gottscho.[5]

Collisions can rapidly transfer population from the pumped to unpumped Λ doublet, and thus provide a mechanism for the appearance of symmetry-forbidden lines even in the absence of an external electric field. Consequently, the results of laser diagnostic experiments will have to be corrected for collisional effects before quantitative values of local electric fields can be extracted. The goal of the present article is to develop the formal framework to allow accurate modeling of these collisional effects. To do so we shall draw heavily on our recent work[6–8] on the theory of inelastic collisions of open-shell molecules. Our description of how collisions modify the field-dependent excitation and fluorescence will involve irreducible multiple moments[9–11] of the excited state density matrix, which, as pointed out by several authors,[10–15] is the natural framework for the study of processes in which polarized radiation is used for both state selection and detection. As a companion to the accompanying paper by Mandich, Gaebe, and Gottscho,[5] describing experimental work on the BCl($A\ ^1\Pi$) molecule in a plasma environment, the present article is an initial theoretical investigation in this area, and will explicitly ignore both hyperfine effects as well as quantum coherences between the various initially excited levels.

The organization of this article is as follows: In the next section we develop the equations describing the initial density matrix and fluorescence intensities for a $^1\Pi$ molecule in an electric field. We go beyond the initial work of Gottscho *et al.*[1] by introducing the multipole moments of the excited state density matrix. The time evolution of the density matrix is discussed in Sec. III. Then, in Sec. IV we analyze the behavior of the fluorescence intensity for both the "forbidden" and allowed lines in the limit of low pressure or low field. The results of a numerical simulation study are presented in Sec. V. This is followed by a brief discussion of quantum coherences and hyperfine effects, and then a conclusion.

II. ABSORPTION AND EMISSION OF A $^1\Pi$ MOLECULE IN THE PRESENCE OF AN ELECTRIC FIELD

In a Hund's case (a) description[16] the wave function for a rotating diatomic molecule in a $^1\Pi$ electronic state is[2]

$$|JM\ ^1\Pi_{e/f}\rangle = |JM\ ^1\Pi\epsilon\rangle = 2^{-1/2}[|JM\Lambda\rangle|\Lambda\rangle + \epsilon|JM-\Lambda\rangle|-\Lambda\rangle], \quad (1)$$

where $|\Lambda\rangle$ is the electronic wave function with Λ being the projection of the electronic orbital angular momentum along the molecular axis (Λ = 1 for an electronic state of Π symmetry), and $|JM\Lambda\rangle$ is the wave function describing the overall rotation of the molecule. Here J is the total angular momentum with space- and molecule-frame projection quantum numbers M and Λ, respectively. The symmetry index ϵ in Eq. (1) can take on the values ± 1. In conventional spectroscopic notation[17] the $\epsilon = +1$ levels are labeled e with total parity $+(-1)^J$ while the $\epsilon = -1$ levels are labelled f with total parity $-(-1)^J$. At high J the electronic wave function is *symmetric* with respect to reflection in the plane of rotation of the molecule for the $e(\epsilon = +1)$ levels and *antisymmetric* for the $f(\epsilon = -1)$ levels.[2] The splitting

 0021-9606/85/193340-09$02.10

between the e and f Λ-doublet levels is equal to $qJ(J+1)$ where q is the Λ-doubling constant, which may be positive or negative.[16] By convention[16] for positive (negative) q the e level lies above (below) the f level.

The presence of an electric field of strength F, which we take to define the space-frame Z axis, introduces an additional term into the molecular Hamiltonian of magnitude $\boldsymbol{\mu}\cdot\mathbf{F}$ where μ is the electric dipole moment of the molecule. This term breaks the reflection symmetry and thereby mixes the e and f Λ-doublet levels of a given J and M.[18,19] Using standard expressions for the electric dipole matrix elements,[20] one can show that the matrix elements of the Stark Hamiltonian are[1]

$$\langle J'M'\,{}^1\Pi\epsilon'|\boldsymbol{\mu}\cdot\mathbf{F}|JM\,{}^1\Pi\epsilon\rangle = \delta_{\epsilon,-\epsilon'}\delta_{MM'}\mu MF/[J(J+1)]. \quad (2)$$

For relatively weak fields the Stark mixing between rotational levels of *different* J will be negligibly small compared to the intradoublet mixing, since the Λ-doublet splitting is much smaller than the rotational energy spacing. In this case the molecular Hamiltonian including the Stark term can be rediagonalized analytically, with the original Λ-doublet wave functions replaced by

$$|JM\,{}^1\Pi F_1\rangle = \cos\theta_{JM}|JM\,{}^1\Pi_e\rangle + \sin\theta_{JM}|JM\,{}^1\Pi_f\rangle \quad (3)$$

and

$$|JM\,{}^1\Pi F_2\rangle = -\sin\theta_{JM}|JM\,{}^1\Pi_e\rangle + \cos\theta_{JM}|JM\,{}^1\Pi_f\rangle, \quad (4)$$

where

$$\theta_{JM} = \tfrac{1}{2}\tan^{-1}\{2\mu MF/q[J(J+1)]^2\}. \quad (5)$$

The angle θ_{JM} ranges from 0 (in the zero-field limit) either up to $\pi/4$ or down to $-\pi/4$, depending on the sign of M and q. Note that $|\theta_{JM}|$ is independent of the sign of M. The F_1 level is nominally e in character and the F_2 level, nominally f.

The absorption of radiation in a ${}^1\Sigma^+ \rightarrow {}^1\Pi$ transition will be proportional to the strength of the transition dipole matrix element. This can be determined from the basic expression[20]

$$\langle J''M''\,{}^1\Sigma^+|Q_m|JM\,{}^1\Pi e\rangle = (-1)^{J''-M''}\begin{pmatrix} J'' & 1 & J \\ -M'' & m & M\end{pmatrix}\langle J''\,{}^1\Sigma\|Q\|J\,{}^1\Pi\epsilon\rangle, \quad (6)$$

where Q_m designates the electric dipole moment operator with m being the circular polarization of the photon with respect to the space-frame Z axis, which is here defined to be the direction of the Stark field. The reduced matrix element is[20]

$$\langle J''\,{}^1\Sigma\|Q\|J\,{}^1\Pi\epsilon\rangle = \sqrt{2}(-1)^{J''}[(2J+1)(2J''+1)]^{1/2} \times\mu_{\Sigma\Pi}[1+\epsilon(-1)^{J+J''+1}]\begin{pmatrix} J'' & 1 & J \\ 0 & -1 & 1\end{pmatrix}, \quad (7)$$

where $\mu_{\Sigma\Pi}$ is the electronic transition moment. The presence of the phase factor in square brackets in Eq. (7) is responsible for the selection rule that in the absence of an electric field P- and R-branch transitions ($J'' = J \mp 1$) will populate only the e Λ-doublet level ($\epsilon = +1$) in the excited state, and Q-branch transitions ($J'' = J$), only the f level.

In the presence of an electric field the e and f levels are mixed, as expressed in Eqs. (3) and (4). If the bandwidth of the pump laser is narrower than the Λ-doublet splitting, then only one of the F_i levels will be excited. For simplicity, we shall treat the case of an F_1 level excited by a P-branch line, although the following development can be easily extended to the other possible situations.

As stated in the Introduction in the present article we shall explicitly ignore all off-diagonal elements,[10,11] (coherences) of the excited state density matrix. The diagonal elements (populations) will be given by

$$\rho_{JMF_1} \sim \sum_{M''} |\langle J''M''\,{}^1\Sigma^+|Q_m|JM\,{}^1\Pi F_1\rangle|^2. \quad (8)$$

In the case of P-branch excitation and a pump laser polarized parallel to the field, Eqs. (3), (6), and (7) can be used to write Eq. (8) as

$$\rho_{JMF_1} \sim \cos^2\theta_{JM} G_{J,J+1}\sum_{M''} H_{JM,J+1M''}(\|), \quad (9)$$

where the Hönl–London factor[16] is

$$G_{J,J''} = (2J+1)(2J''+1)\begin{pmatrix} J'' & 1 & J \\ 0 & -1 & 1\end{pmatrix}^2 \quad (10)$$

and where

$$H_{JM,J''M''}(\|) = \delta_{MM''}\begin{pmatrix} J'' & 1 & J \\ -M & 0 & M\end{pmatrix}^2. \quad (11)$$

In the case of polarization perpendicular to the field a similar expression is obtained, except that the $H_{JM,J'M''}$ factor is replaced by

$$H_{JM,J''M''}(\perp) = \frac{1}{2}\left[\begin{pmatrix} J'' & 1 & J \\ -M'' & 1 & M\end{pmatrix}^2 + \begin{pmatrix} J'' & 1 & J \\ -M'' & -1 & M\end{pmatrix}^2\right]. \quad (12)$$

Note that the individual populations of each M level are independent of the sign of M. Field parallel and field perpendicular transitions are often denoted π and σ transitions, respectively.[21]

If, however, the bandwidth of the pump laser is *larger* than the Λ-doublet splitting, then both the F_1 and F_2 levels will be excited, so that we must add to Eq. (9) an expression for the diagonal elements of the density matrix of the F_2 level. This expression is from Eq. (4)

$$\rho_{JMF_2} \sim \sin^2\theta_{JM} G_{J,J+1}\sum_{M''} H_{JM,J+1M''}(\| \text{ or } \perp), \quad (13)$$

which we see to be exactly the same as Eq. (8), except with the $\cos^2\theta_{JM}$ factor replaced by $\sin^2\theta_{JM}$. In the limit of zero field, $\theta_{JM} = 0$, and, as expected, only the F_1 level will be excited by a P-branch line. We observe also that for broadband excitation the total excited state population ($\rho_{JMF_1} + \rho_{JMF_2}$) is independent of the strength of the external field.

It will be convenient to work with the *multipole moments*[9–15] of the excited state density matrices, which are defined by [9]

$$\rho^K_{JF_i} = (-1)^{K-J}(2K+1)^{1/2}\sum_M (-1)^{-M} \times \begin{pmatrix} J & J & K \\ -M & M & 0 \end{pmatrix} \rho_{JMF_i}. \quad (14)$$

Substitution of Eq. (8) gives

$$\rho^K_{JF_1} = (-1)^{K-J}(2K+1)^{1/2} G_{J,J+1} \sum_{MM'} (-1)^{-M} \times H_{JM,J+1M'} \begin{pmatrix} J & J & K \\ -M & M & 0 \end{pmatrix} \cos^2\theta_{JM}. \quad (15)$$

The expression for $\rho^K_{JF_2}$ is identical, except with the $\cos^2\theta_{JM}$ factor replaced by $\sin^2\theta_{JM}$.

In the zero-field limit $\theta_{JM} = 0$ and the summation in Eq. (15) can be evaluated to give, for $\|$ excitation,

$$\rho^K_{JF_1}(F=0) = -(2K+1)^{1/2} G_{J,J+1} \times \begin{pmatrix} 1 & 1 & K \\ 0 & 0 & 0 \end{pmatrix} \begin{Bmatrix} 1 & 1 & K \\ J & J & J+1 \end{Bmatrix}, \quad (16)$$

and, for $\perp$ excitation,

$$\rho^K_{JF_1}(F=0) = \tfrac{1}{2}(2K+1)^{1/2} G_{J,J+1}[1+(-1)^K] \times \begin{pmatrix} 1 & 1 & K \\ 1 & -1 & 0 \end{pmatrix} \begin{Bmatrix} 1 & 1 & K \\ J & J & J+1 \end{Bmatrix}. \quad (17)$$

From the properties[9] of the $3j$ symbols in Eqs. (16) and (17) we deduce, as is well known,[10,11] that for linearly polarized light, only *population* ($K=0$) and *alignment* ($K=2$) can be created in the excited state. In the presence of an electric field higher tensor multipoles can be created, although, because the ρ_{JMF_i} are independent of the sign of M, the symmetry properties of the $3j$ symbol in Eq. (14) imply that these higher moments will be limited to even values of K. We observe, however, that for broadband excitation, the sum of $\rho^K_{JF_2}$ and $\rho^K_{JF_1}$ will be independent of field strength, and given by Eqs. (16) or (17). Since the $3j$ symbol in Eqs. (16) and (17) vanishes for $K>2$, it follows that

$$\rho^K_{JF_1} = -\rho^K_{JF_2} \quad \text{for} \quad K>2. \quad (18)$$

It will be useful below to derive limiting expressions for the multipole moments of the F_1 and F_2 density matrices, valid when the field is weak. For F small, the angle θ_{JM} in Eq. (5) will be small, so that

$$\theta_{JM} \simeq \mu MF/q[J(J+1)]^2, \quad (19)$$

leading to

$$\cos^2\theta_{JM} = 1 - (\mu MF/q)^2[J(J+1)]^4 + O(F^4) \quad (20)$$

and

$$\sin^2\theta_{JM} = (\mu MF/q)^2[J(J+1)]^4 + O(F^4). \quad (21)$$

Substituting Eq. (20) into Eq. (15), and making use of the relation[21]

$$\begin{pmatrix} J & J & 1 \\ -M & M & 0 \end{pmatrix}^2 = M^2/[J(J+1)(2J+1)], \quad (22)$$

we find

$$\rho^K_{JF_1} = \rho^K_{JF_1}(F=0) - (\mu F/q)^2 \bar{\rho}^K_J + O(F^4), \quad (23)$$

where the zero-field multipole moments are defined by Eqs. (16) or (17) and

$$\bar{\rho}^K_J = (-1)^{K-J} \frac{(2K+1)^{1/2}(2J+1)G_{J,J+1}}{[J(J+1)]^3} \times \sum_{MM'} (-1)^{-J-M} H_{JM,J+1M'} \times \begin{pmatrix} J & J & 1 \\ -M & M & 0 \end{pmatrix}^2 \begin{pmatrix} J & J & K \\ -M & M & 0 \end{pmatrix}. \quad (24)$$

Similarly, by substitution of Eq. (21) we find

$$\rho^K_{JF_2} = (\mu F/q)^2 \bar{\rho}^K_J + O(F^4). \quad (25)$$

As anticipated, Eqs. (23) and (25) satisfy Eq. (18).

The time evolution of the individual multipole moments of the excited state density matrix will be described in the next section. Physically, collisions can redistribute population between the F_1 and F_2 levels, or between the M levels in a given Λ-doublet level. Concurrently the excited state can fluoresce. For fluorescence on a P- or R-branch line the total oscillator strength will arise from the e components in the F_1 and F_2 levels, and for a Q-branch line, from the f components. Regardless of the bandwidth of the pump laser, we shall assume that the Λ doublet and Stark splitting in the excited state is much less than the bandpass of the spectrometer.

If $\rho_{JMF_i}(t)$ denotes the diagonal density matrix elements at a time t after the initial excitation, then from Eqs. (3), (4), and (8)–(13), we can obtain the following expression for the total R-branch emission intensity:

$$I_R(t, \| \text{ or } \perp) \sim G_{J,J-1} \sum_{MM'} H_{JM,J-1M'}(\| \text{ or } \perp) \times [\cos^2\theta_{JM}\,\rho_{JMF_1}(t) + \sin^2\theta_{JM}\,\rho_{JMF_2}(t)]. \quad (26)$$

Each JMF_i level will radiate with probability proportional to the product of line-strength factors ($G_{J,J'}$ and $H_{JM,J'M'}$) and the fractional e character, expressed by the $\cos^2\theta_{JM}$ and $\sin^2\theta_{JM}$ factors in Eqs. (3) and (4). The total intensity is the sum over all contributing levels. For P-branch emission the $J-1$ indices are replaced by $J+1$. However, for Q-branch emission the total oscillator strength is proportional to the fractional f character in both the F_1 and F_2 levels so that Eq. (26) is replaced by

$$I_Q(t, \| \text{ or } \perp) \sim G_{J,J} \sum_{MM'} H_{JM,JM'}(\| \text{ or } \perp) \times [\sin^2\theta_{JM}\,\rho_{JMF_1}(t) + \cos^2\theta_{JM}\,\rho_{JMF_2}(t)]. \quad (27)$$

The above expressions for the fluorescence intensity [Eqs. (26) and (27)] can be recast in terms of the multipole moments of the excited state density matrices by using the inverse[9] of Eq. (14). We find

$$I_R(t,\parallel \text{ or } \perp) \sim G_{J,J-1} \sum_K (2K+1)^{1/2}(-1)^{K-J} \sum_{MM'} (-1)^{-M} \times H_{JM,J-1M'}(\parallel \text{ or } \perp) \begin{pmatrix} J & J & K \\ -M & M & 0 \end{pmatrix} \times [\cos^2\theta_{JM}\,\rho^K_{JF_1}(t) + \sin^2\theta_{JM}\,\rho^K_{JF_2}(t)]. \tag{28}$$

The expression for the Q-branch intensity is identical to Eq. (28) with the $\cos^2\theta_{JM}$ and $\sin^2\theta_{JM}$ factors reversed.

III. TIME EVOLUTION OF THE EXCITED STATE DENSITY MATRIX

The time evolution of the diagonal elements of the density matrix of the excited Λ-doublet level is described by the following master equation:[11,14]

$$\dot\rho_{JMF_1} = -\Gamma\rho_{JMF_1} - \sum_{M'} [(R_{JMF_1\to JM'F_1} + R_{JMF_1\to JM'F_2})\rho_{JMF_1} + R_{JM'F_1\to JMF_1}\,\rho_{JM'F_1} + R_{JM'F_2\to JMF_1}\,\rho_{JM'F_2}], \tag{29}$$

and similarly for $\dot\rho_{JMF_2}$. Here Γ is the radiative decay rate which is independent of M since

$$H_{JM,J'M'}(\parallel) + 2H_{JM,J'M'}(\perp) = (2J+1)^{-1}, \tag{30}$$

which follows from the orthogonality properties[9,22] of the $3j$ symbols in Eqs. (11) and (12). The thermal rates in Eq. (29) are defined by

$$R_{JMF_i\to JM'F_j} = \rho_T \int v\sigma_{JMF_i\to JM'F_j}(v) f(v) dv, \tag{31}$$

where ρ_T designates the number density of collision partners and the integral extends over a Maxwellian distribution of relative velocities. As stated earlier, we are explicitly ignoring coherence effects, which would necessitate[10,11] including the off-diagonal terms of the excited state density matrix in a generalized master equation.

We have shown earlier[23] how the M-resolved cross sections in Eq. (31) can be written in terms of *tensor opacities*, namely,

$$\sigma_{JMF_i\to JM'F_j}(v) = \frac{\pi}{k_J^2} \sum_{K_1Q_1} \begin{pmatrix} J & J & K_1 \\ -M & M' & -Q \end{pmatrix}^2 P^{K_1}_{JF_i,JF_j}(v), \tag{32}$$

where k_J is the wave vector in the initial channel. The tensors opacities arise from a spherical tensor expansion of the scattering T matrix,[10,24–28] in a coupling scheme first introduced into the field of molecular collisions by Curtiss, Snider, and co-workers[25] and into the field of atomic collisions by Grawert.[26] The degeneracy averaged cross section for the $JF_i\to JF_j$ transition is given by[24]

$$\sigma_{JF_i\to JF_j} = \frac{\pi}{(2J+1)k_J^2} \sum_{K_1} P^{K_1}_{JF_i,JF_j}. \tag{33}$$

Now, if we introduce Eqs. (31) and (32) into Eq. (29), multiply both sides by $(-1)^{J+M}\begin{pmatrix} J & J & K \\ -M & M & 0 \end{pmatrix}$, sum over M, and make use of Eq. (14), we can obtain, with some angular momentum algebra, an equation for the time evolution of the multipole moments of the excited state density matrix. We find

$$\dot\rho^K_{JF_1} = -(\Gamma + R^0_{JF_1,JF_1} - R^K_{JF_1,JF_1} + R^0_{JF_1,JF_2}) \times \rho^K_{JF_1} + R^K_{JF_2,JF_1}\,\rho^K_{JF_2}, \tag{34}$$

and similarly for $\dot\rho^K_{JF_2}$. Here the quantity $R^K_{JF_i,JF_j}$ is a multipole rate, given by

$$R^K_{JF_i,JF_j} = \frac{\pi\rho_T}{k_J^2} \int \sum_{K_1} (-1)^{K_1+K} \times \begin{Bmatrix} J & J & K \\ J & J & K_1 \end{Bmatrix} P^{K_1}_{JF_i,JF_j} v f(v) dv. \tag{35}$$

Alexander and Orlikowski[8] have defined, in analogy with the practice in nuclear physics,[29] a *multipole transfer efficiency* which indicates the degree to which the K th multipole of the initial density matrix, normalized to the zeroth moment, is preserved by a collision. This can be easily extended to thermal rates. If we define a *tensor rate*

$$V^{K_1}_{JF_i,JF_j} \equiv \frac{\pi\rho_T}{k_J^2} \int P^{K_1}_{JF_i,JF_j} v f(v) dv, \tag{36}$$

then

$$R^K_{JF_i,JF_j} = E^K_{JF_i,JF_j}\,R^0_{JF_i,JF_j}, \tag{37}$$

where the multipole transfer efficiency is given by

$$E^K_{JF_i,JF_j} = (-1)^{K-2J}(2J+1) \times \frac{\sum_{K_1} (-1)^{K_1} \begin{Bmatrix} J & J & K \\ J & J & K_1 \end{Bmatrix} V^{K_1}_{JF_i,JF_j}}{\sum_{K_1} V^{K_1}_{JF_i,JF_j}}. \tag{38}$$

Because of the orthogonality properties of the 6j symbols,[19] one can show that $E^K_{JF_i,JF_j} \leqslant 1$.

This development allows us to write Eq. (34) as

$$\dot\rho^K_{JF_1} = -[\Gamma + R^0_{JF_1,JF_1}(1 - E^K_{JF_1,JF_1}) + R^0_{JF_1,JF_2}]\,\rho^K_{JF_1} + R^K_{JF_2,JF_1}\,\rho^K_{JF_2}. \tag{39}$$

This is quite similar to an analogous rate equation given by Omont,[10,30] with the inclusion here of both Λ-doublet levels. The four terms of the right-hand side of Eq. (39) have the following simple physical interpretation: The first is an overall loss term due to radiative decay, the second expresses the loss of polarization in the F_1 manifold due to M-changing collisions within the F_1 manifold, the third is a loss term (independent of K) due to inelastic transitions *into* the other Λ-doublet level ($F_1\to F_2$), and, finally, the fourth term expresses the change in the K th moment of the density matrix due to inelastic transitions *from* the other (F_2) Λ-doublet level.

We observe that the time evolution of each multipole moment of the excited state density matrix is uncoupled from that of every other moment. This is well-known,[7,10,13,14,31] and a consequence of the assumed isotropy of the distribution of relative velocity vectors with respect to the laboratory-frame coordinate system. *This uncoupling is a tremendous simplification*, reducing the initial set of coupled rate equations of dimensionality $4J+2$ [Eq. (29)] to $2J+1$ sets of two coupled equations [Eq. (39)].

Since the tensor opacities are symmetric in the initial and final indices, and assuming that the Λ-doublet and Stark splittings are negligibly small compared to the average translational energy, we have

$$R^K_{JF_i,JF_j} = R^K_{JF_j,JF_i}. \tag{40}$$

In addition we shall assume that

$$R^K_{JF_i,JF_i} = R^K_{JF_j,JF_j}. \tag{41}$$

Although this latter equality will not be rigorous in the case of a $^1\Pi$ molecule,[6,32,33] the difference between the two rates will probably not be large, so that Eq. (41) is a reasonable assumption, especially in the absence of quantitative knowledge of these rates.

With Eqs. (40) and (41) we can solve analytically Eq. (39) as well as the analogous equation for $\dot{\rho}_{JF_2}$. We find

$$\rho^K_{JF_i}(t) = \tfrac{1}{2}e^{-\Gamma t}e^{-A^K_J t}\{\rho^K_{JF_i}(t=0) + \rho^K_{JF_j}(t=0) + [\rho^K_{JF_i}(t=0) - \rho^K_{JF_j}(t=0)]e^{-2B^K_J t}\}, \tag{42}$$

where

$$A^K_J = R^0_{JF_i,JF_i}(1 - E^K_{JF_i,JF_i}) + R^0_{JF_j,JF_i}(1 - E^K_{JF_j,JF_i}) \tag{43}$$

and

$$B^K_J = R^K_{JF_j,JF_i} = E^K_{JF_j,JF_i} R^0_{JF_j,JF_i}. \tag{44}$$

Note that an analytic solution to Eq. (39) is still possible even if Eq. (41) is not assumed.

Equations (5), (9)–(14), (29), and (42)–(44) provide the means to calculate the time and field dependence of fluorescence emission from a molecule in a laser-excited $^1\Pi$ electronic state, provided that numerical values are given to the relevant spectroscopic and collisional parameters.

IV. LIMITING EXPRESSIONS FOR FLUORESCENCE INTENSITIES

If we introduce Eq. (42) into Eq. (28), or into the similar equation for the Q-branch intensity, we obtain

$$I_{J''}(t,\| \text{ or } \perp) = \tfrac{1}{2}e^{-\Gamma t}G_{J,J''}\sum_{KMM''}(-1)^{K-J-M}(2K+1)^{1/2} \times e^{-A^K_J t}\begin{pmatrix} J & J & K \\ -M & M & 0\end{pmatrix} H_{JM,J''M''}(\| \text{ or } \perp) \times \{\rho^K_{JF_1}(t=0) + \rho^K_{JF_2}(t=0) - (-1)^{J+J''}e^{-2B^J_K t}[\rho^K_{JF_1}(t=0) - \rho^K_{JF_2}(t=0)]\cos 2\theta_{JM}\}, \tag{45}$$

where $J'' = J-1, J$, or $J+1$ for, respectively, R-, Q-, and P-branch fluorescence. Before proceeding to numerical simulation studies, it is worthwhile to derive simplified expressions for Eq. (45) in the zero-field as well as zero-collision (low pressure) limits.

In the zero-field limit $\theta_{JM} = 0$, $\rho^K_{JF_2} = 0$, and $\rho^K_{JF_1}$ is given by either Eq. (16) or Eq. (17). Equation (45) can then be reduced to

$$I_{J''}(t,\|) = (-1)^{J+J''}\tfrac{1}{2}e^{-\Gamma t}G_{J,J''}\sum_K (2K+1)^{1/2}e^{-A^K_J t} \times [1-(-1)^{J+J''}e^{-2B^K_J t}] \times \rho^K_{JF_1}(F=0)\begin{pmatrix}1 & 1 & K\\ 0 & 0 & 0\end{pmatrix}\begin{Bmatrix}1 & 1 & K\\ J & J & J''\end{Bmatrix}, \tag{46}$$

with a similar expression in the case of perpendicular polarization. In the short-time (or low pressure) limit, one can expand the exponentials to obtain the following expression for the ratio of the Q-branch to R-branch intensities:

$$\lim_{t \text{ small}} \frac{I_Q(\|)}{I_R(\|)} = \frac{-G_{J,J}\sum_K (2K+1)^{1/2}B^K_J\rho^K_{JF_1}(F=0)\begin{pmatrix}1 & 1 & K\\ 0 & 0 & 0\end{pmatrix}\begin{Bmatrix}1 & 1 & K\\ J & J & J\end{Bmatrix}}{G_{J,J-1}\sum_K (2K+1)^{1/2}\rho^K_{JF_1}(F=0)\begin{pmatrix}1 & 1 & K\\ 0 & 0 & 0\end{pmatrix}\begin{Bmatrix}1 & 1 & K\\ J & J & J-1\end{Bmatrix}}t, \tag{47}$$

which is linear in time. The comparable expression in the case of $\perp$ polarization is identical except that the $3j$ symbol $\left(\begin{smallmatrix}1 & 1 & K\\ 0 & 0 & 0\end{smallmatrix}\right)$ is replaced by $\frac{1}{2}[1+(-1)^K]\left(\begin{smallmatrix}1 & -1 & K\\ 1 & 0 & 0\end{smallmatrix}\right)$.

We turn now to an expression for the fluorescence intensity, valid at low fields and at low pressure. To do so we set $t=0$ in Eq. (45) and assume F small, so that we can use Eqs. (19)–(25). We obtain

$$I_{J''}(\| \text{ or } \perp) = \tfrac{1}{2}G_{JJ''}\sum_{KMM''}(-1)^{K-J-M}(2K+1)^{1/2} \times \begin{pmatrix} J & J & K\\ -M & M & 0\end{pmatrix} H_{JM,J''M''} \times \{[1-(-1)^{J+J''}]\rho^K_{JF_1}(F=0) + 2(-1)^{J+J''}(\mu F/q)^2[\bar{\rho}^K_J + \rho^K_{JF_1}(F=0) \times M^2/J^4(J+1)^4] + O(F^4)\}, \tag{48}$$

where $\rho^K_{JF_1}(F=0)$ is defined by Eq. (16) or (17), and $\bar{\rho}^K_J$ by Eq. (24). The presence of the factor $[1-(-1)^{J+J''}]$ implies that for R-branch emission the leading term is independent of the field, while for Q-branch emission the leading term varies quadratically with the field strength. Thus we predict at low fields

$$I_Q/I_R \sim F^2. \tag{49}$$

The constant of proportionality will depend on both the excitation and detection polarization. The explicit expressions are complicated and will not be given here.

V. MODEL STUDIES OF COLLISIONAL EFFECTS ON FLUORESCENCE INTENSITIES

To gain further insight it is necessary to carry out simulation studies based on Eq. (45). The electric field will be defined in reduced units

$$\mathscr{F} = \mu F/q, \tag{50}$$

where μ,F, and q are assumed to be in atomic units. If μ is measured in Debye, q in cm^{-1}, and F in V/cm, then the correct conversion is

$$\mathscr{F} = 1.6792\times 10^{-5}\,\mu(\mathrm{D})\,F(\mathrm{V/cm})/q(\mathrm{cm}^{-1}). \tag{51}$$

Exact values for the collisional parameters which define the A_J^K and B_J^K rates [Eqs. (43) and (44)] can be obtained from converged quantum calculations of the relevant cross sections based on accurate potential surfaces.

For the present model studies we shall be guided by the work of Mandich *et al.* and take the $K = 0$ elastic ($F_i = F_j$) rate to be six times the $K = 0$ rate for $F_1 \rightarrow F_2$ transitions. We estimate the latter (R_{JF_1,JF_2}) to be $7.9\times 10^5\ s^{-1}$ for $J = 5$ and $5.6\times 10^5\ s^{-1}$ for $J = 11$ by using the experimental estimate of Mandich, Gaebe, and Gottscho[5] of the degeneracy averaged intra-Λ-doublet transfer rate constants (see Table II of Ref. 5), and by assuming a target gas pressure of 0.3 Torr.

Based on the results of our recent calculation[8] of depolarization cross sections in collisions of Ar with NO in the lower ($\Omega = 1/2$) spin-orbit, rotational manifold of the ground electronic state ($X\,^2\Pi$), we shall assume that elastic ($F_i = F_j$) depolarization is inefficient, so that the elastic multipole transfer efficiencies will be close to unity. We take

$$E^K_{JF_i,JF_i} = 0.9, \quad K = 1,2,\ldots . \tag{52}$$

However, to judge from the same calculations,[8] depolarization will be much stronger for the Λ = doublet *changing* transitions ($F_i \neq F_j$). The following reasoning will be used to assign values to these parameters: First, as discussed in several previous papers[7,8] we anticipate that for e/f changing transitions the tensor opacities [Eqs. (32), (33), and (35)] for a molecule with odd multiplicity will vanish unless K_1 = odd. Secondly, our Ar–NO calculations suggest that these nonvanishing tensor opacities (of number J) will be roughly independent of K_1. This suggests that a reasonable approximation will be to take the $F_1 \rightarrow F_2$ *tensor rates* [Eq. (36)] to be constant (for K_1 = odd) and given by

$$V^{K_1}_{JF_i,JF_{j\neq i}} = \frac{2J+1}{J} R^0_{JF_i,JF_{j\neq i}}, \tag{53}$$

where in the present application $R^0_{JF_i,JF_{j\neq i}} = 7.9\times 10^5\ s^{-1}$ for $J = 5$ or $5.6\times 10^5\ s^{-1}$ for $J = 11$, as discussed above. The factor of $(2J+1)/J$ in Eq. (53) ensures that the sum over K_1 satisfies statistical microreversibility, as implied by Eqs. (33) and (36).

A perhaps more realistic set of inelastic ($F_1 \rightarrow F_2$) tensor rates can be derived from the new scaling relation for M-dependent transitions in collisions of open-shell molecules developed by Derouard.[33] We find (for K_1 odd),

$$V^{K_1}_{JF_i,JF_{j\neq i}} = N_J(2J+1)R^0_{JF_i,JF_{j\neq i}} \begin{pmatrix} J & J & K_1 \\ -1 & 1 & 0 \end{pmatrix}^2 / (K_1 + \tfrac{1}{2}), \tag{54}$$

where the normalization constant N_J is chosen so that the sum over K_1 satisfies statistical microreversibility.

Figure 1 displays the ratio of Q- to R- branch fluorescence intensities as a function of reduced field strength for parallel polarized excitation and for both parallel and perpendicular detection. Broadband excitation of both the F_1 and F_2 levels for $J = 5$ and $J = 11$ is assumed. Curves are shown corresponding to times of 0,20, and 50 ns after excitation, or alternatively to a time of 10 ns and pressures of 0,0.6, and 1.5 Torr. Complementary insight into the role of colli-

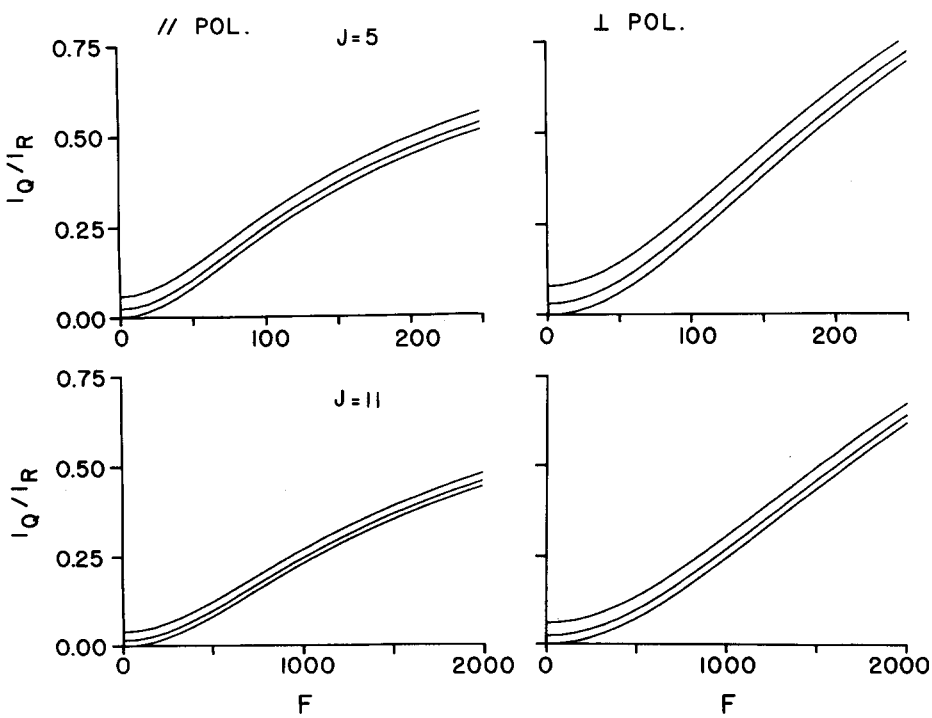

FIG. 1. Ratio of Q- to R-branch fluorescence intensities subsequent to excitation of the $J = 5$ (upper two panels), or $J = 11$ (lower two panels) Λ-doublet levels, as a function of electric field strength in reduced units [see Eq. (51)]. The left-hand panels correspond to fluorescence polarization parallel to the electric field; the right-hand panels, to fluorescence polarization perpendicular to the field. In all cases P-branch excitation with parallel polarization is assumed. The bandwidth of the pump laser is assumed to be larger than the Λ-doublet splitting, so that both Λ-doublet levels are initially excited, in proportion to the fractional e character in each of the F_1 and F_2 levels. The three curves displayed in each panel correspond, from bottom to top, to times of 0, 20, and 50 ns after excitation; the underlying collisional parameters are described in Sec. V. To within the resolution of the plots, the curves are insensitive to the specific choice of collisional transfer rates [Eqs. (53) or (54)].

sions is provided by Fig. 2, where the Q- to R-branch fluorescence intensities are plotted as a function of time after initial excitation for fixed field. The time scale investigated is appropriate to the BCl ($A\ ^1\Pi$) radical, used in the experiments of Gottscho *et al.*,[1,5] with a radiative lifetime of 19 ns.

Qualitatively the behavior is as predicted in Sec. IV: a linear dependence on t and a quadratic dependence on F, at least in the low-field limit. Because the Λ-doublet splitting increases, and the Stark mixing *decreases*, as $J(J+1)$, the onset of the "forbidden" Q-branch lines shifts dramatically to higher field as J increases. Obviously, the predicted intensity ratios will be strongly dependent on the $K=0$ $F_1 \rightarrow F_2$ population transfer rate $R^0_{JF_iJF_{j\neq i}}$. To judge from the linear dependence on t seen in Fig. 2 and in Eq. (47), we anticipate a linear dependence on $R^0_{JF_iJF_{j\neq i}}$.

As already anticipated by Gottscho *et al.*,[1] the dependence on field of the Q- to R-branch intensity ratio is more pronounced in the case of perpendicular detection. It is interesting that this is also true of the variation with collision time (or, equivalently, pressure), as can be seen clearly in Fig.2. This dependence on the direction of polarization of the fluorescence is more marked at higher J. To investigate further this polarization dependence we plot in Fig. 3 the time dependence, for several values of the electric field, of the linear polarization of the fluorescence, defined by[10,11]

$$P=[I(\|)-I(\perp)]/[I(\|)+I(\perp)]. \tag{55}$$

For both P- and R-branch excitation, in the zero-field limit the linear polarization of the "allowed" line can be shown[10] to be 1/7, independent of J. We observe that this polarization is shifted upward slightly in the presence of an electric field, and that this shift is more pronounced for $J=11$ than $J=5$. The small degree of dependence on electric field is explained by Eq. (48), which reveals, as discussed in Sec. IV, that for allowed emission the leading term in the expression for both the parallel and perpendicular intensity is independent of the field. By contrast, the linear polarization of the forbidden line appears to be very sensitive to the strength of the electric field. Additionally, as illustrated in the four upper panels of Fig. 3, the polarization of the forbidden line varies significantly when an R branch, rather than a P branch, is used to populate the excited state. This is because for R-branch, parallel polarized excitation the $\Delta M=0$ selection rule does not allow population of the

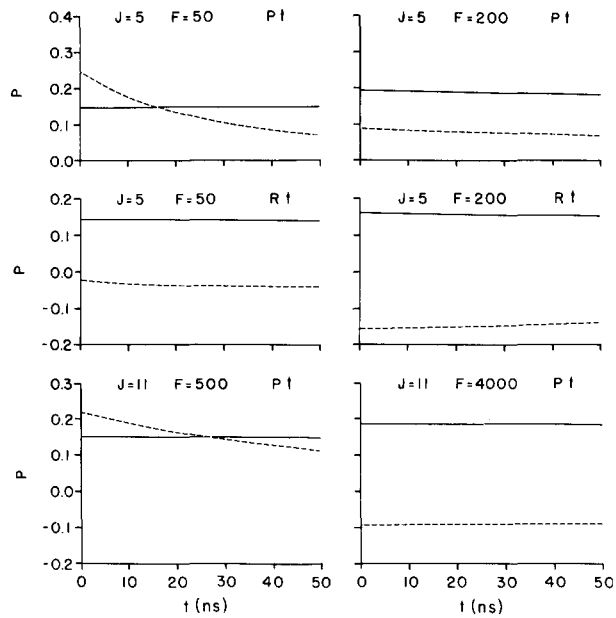

FIG. 3. Linear polarization $[P=(I_\| - I_\perp)/(I_\| + I_\perp)]$ of Q-branch fluorescence (dashed lines) and R-branch (or P-branch) fluorescence (solid lines) subsequent to excitation of the $J=5$ or $J=11$ Λ-doublet levels, as a function of time. The field strengths are given in reduced units [Eq. (51)]. The bandwidth of the pump laser is assumed to be larger than the Λ-doublet splitting, so that both Λ-doublet levels are initially excited, in proportion to the fractional e character in each of the F_1 and F_2 levels. In the top and bottom panels the excitation is P-branch and the solid curves correspond to R-branch fluorescence. The situation is reversed in the middle two panels; R-branch excitation and P-branch fluorescence. In all cases parallel polarization is assumed for the excitation photon.

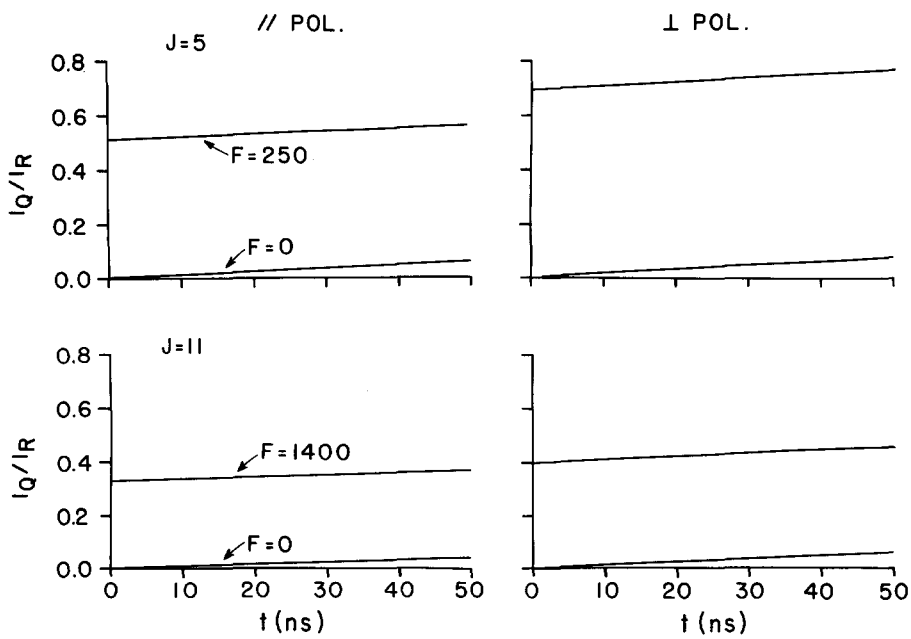

FIG. 2. Ratio of Q- to R-branch fluorescence intensities subsequent to excitation of the $J=5$ (upper two panels) and $J=11$ (lower two panels) Λ-doublet levels, as a function of time. In each panel the two traces correspond to different field strengths [given in reduced units, see Eq. (51)]. The left-hand panels correspond to fluorescence polarization parallel to the electric field; the right-hand panels, to fluorescence polarization perpendicular to the field. In all cases P-branch excitation with parallel polarization is assumed. The bandwidth of the pump laser is assumed to be larger than the Λ-doublet splitting, so that both Λ-doublet levels are initially excited, in proportion to the fractional e character in each of the F_1 and F_2 levels.

$M = 5$ levels which are the most strongly Stark mixed with the f Λ-doublet level. Finally, we notice that collisions appear to depolarize the forbidden line fluorescence more efficiently than the allowed line fluorescence, at least over a 50 ns period.

VI. DISCUSSION

As mentioned above, one major omission from the present treatment is the role of coherences,[10,11] especially in the case of broadband excitation. In the absence of collisional effects, radiation from the Stark split levels will be modulated, due to quantum beating, at frequencies equal to the splitting between these levels. For $J = 5$ at a reduced field strength of 150 (see Figs. 1 and 2), and with a Λ-doubling constant of $q = 2.5 \times 10^{-5}$ cm^{-1}, this splitting ranges from 7.5×10^{-4} cm^{-1} for $M = 0$ to 1.5×10^{-3} cm^{-1} for $M = 5$ corresponding to beat frequencies of ~40 MHz. Thus, if the radiative lifetime of the excited state is ~20 ns, we would anticipate being able to observe, even under ideal conditions, only several quantum beats. In practice, observation of these beats will be obscured by interference due to the beating between each pair of Stark mixed M levels and washed out by collisional effects. Thus, the present incoherent treatment should provide an excellent overall description of collisional contributions to Stark mixing for all but the lowest rotational levels.

The marked variation of the polarization of the forbidden line fluorescence with both electric field and the choice of P- or R-branch excitation seen here suggest that polarization measurements could provide a way to measure electric field strength which is complementary to the measurement of the forbidden to allowed fluorescence intensities. However, Mandich *et al.*[5] did not observe any polarization dependence in their Stark experiments on BCl ($A\ ^1\Pi$) in a plasma environment. An explanation might involve depolarization due to the hyperfine splitting[18,34] in a molecule with nonzero nuclear spin. If so, it will be necessary to extend the present theoretical treatment to include hyperfine interactions. We anticipate that this can be done in a straightforward manner, by the addition of an extra degree of vector coupling to the formal development contained in Sec. II and III above. Along similar lines Rowe and McCaffery[35] have discussed the effect of hyperfine coherences on the *circular* polarization of fluorescence from a molecule in a $^1\Sigma_u^+$ electronic state.

VII. CONCLUSION

We have presented here the theoretical framework necessary to describe both inelastic collisions between Stark mixed Λ-doublet levels of a molecule in a $^1\Pi$ electronic state, as well as the subsequent effect on fluorescence intensities. We have carried out simulation studies of field and temporal (pressure) variation of the ratio of fluorescence intensities for emission on forbidden and allowed $^1\Sigma^+ \leftarrow {}^1\Pi$ lines. The choice of collisional parameters used was guided by previous theoretical studies[6–8,33] of inelastic collisions involving molecules in Π electronic states. For weak fields and short times after excitation (or, equivalently, low pressures) the intensity ratios vary linearly with time and quadratically with field, and are insensitive to the detailed choice of collisional cross sections, provided that these values conform to the expected[6–8,33] qualitative behavior for these processes. Additionally, the linear polarization of the forbidden emission appears to be sensitive to the strength of the electric field, as well as to the choice of the initial excitation step, and may provide a useful probe of field strength and anisotropy.

This article will provide the foundation for the more accurate interpretation of, on the one hand, laser diagnostic studies in plasma environments, such as those of Gottscho and co-workers,[1,5] and, on the other hand, laser-fluorescence or double-resonance studies of intra-Λ-doublet transitions under low pressure, uniform field conditions.[36,37] Subsequent theoretical work[38] will be devoted both to a careful study of quantum coherence and hyperfine effects, neglected here but discussed briefly in the preceding section, as well as to the investigation of the effect of the time varying fields which characterize rf discharge plasmas. We anticipate further theoretical and experimental work in this area, which is a bridge between spectroscopy and kinetics with obvious relevance to microelectronics and plasma chemistry.

ACKNOWLEDGMENTS

The work reported here was supported in part by the National Science Foundation, Grant CHE84-05828. The calculations were carried out at the Center for Intensive Computation, University of Maryland, supported in part by a grant to MHA under the DoD University Research Instrumentation Program (grant ARO-DAAG-29-84-G-0078). The author is grateful to Richard Gottscho, Mary Mandich, and Carl Gaebe for their encouragement and for many helpful discussions, and to Jacques Derouard for permission to use his new scaling relation for M-dependent transitions in collisions of open-shell molecules and for pointing out a numerical error in our preliminary calculations.

[1] C. A. Moore, G. P. Davis, and R. A. Gottscho, Phys. Rev. Lett. **52**, 538 (1984).
[2] M. H. Alexander and P. J. Dagdigian, J. Chem. Phys. **80**, 4325 (1984).
[3] R. E. Drullinger, M. M. Hessel, and E. W. Smith, in *Laser Spectroscopy*, edited by S. Haroche, J. C. Pebay-Peyroula, T. W. Hänsch, and S. E. Harris (Springer, Berlin, 1975), p. 91.
[4] C. B. Zarowin, J. Electrochem. Soc. **130**, 1144 (1983); and references therein.
[5] M. L. Mandich, C. E. Gaebe, and R. A. Gottscho, J. Chem. Phys. **83**, 3349 (1985).
[6] M. H. Alexander, J. Chem. Phys. **76**, 5974 (1982).
[7] M. H. Alexander and S. L. Davis, J. Chem. Phys. **79**, 227 (1983).
[8] M. H. Alexander and T. Orlikowski, J. Chem. Phys. **80**, 1506 (1984).
[9] D. M. Brink and G. R. Satchler, *Angular Momentum*, 2nd ed. (Oxford University, Oxford, 1975).
[10] A. Omont, Prog. Quantum Electron. **51**, 69 (1977).
[11] K. Blum, *Density Martix Theory and Applications* (Plenum, New York, 1981).
[12] D. A. Case, G. M. McClelland, and D. R. Herschbach, Mol. Phys. **35**, 541 (1978).
[13] M. D. Rowe and A. J. McCaffery, Chem. Phys. **43**, 35 (1979).
[14] Ph. Bréchignac, A. Picard-Bersellini, R. Charneau, and J. M. Launay, Chem. Phys. **53**, 165 (1980).
[15] M. J. Proctor and A. J. McCaffery, J. Chem. Phys. **80**, 6038 (1984).
[16] G. Herzberg, *Spectra of Diatomic Molecules*, 2nd ed. (Van Nostrand, Princeton, 1968).
[17] J. M. Brown, J. T. Hougen, K.-P. Huber, J. W. C. Johns, I. Kopp, H.

Lefebvre-Brion, A. J. Merer, D. A. Ramsay, J. Rostas, and R. N. Zare, J. Mol. Spectrosc. **55**, 500 (1975).
[18]A. Carrington, D. H. Levy, and T. A. Miller, Adv. Chem. Phys. **18**, 149 (1970).
[19]R. W. Field and T. H. Bergeman, J. Chem. Phys. **54**, 2936 (1971).
[20]M. H. Alexander, J. Chem. Phys. **76**, 429 (1982).
[21]C. H. Townes and A. L. Schawlow, *Microwave Spectroscopy* (McGraw-Hill, New York, 1955), p. 287.
[22]A. R. Edmonds, *Angular Momentum in Quantum Mechanics* (Princeton University, Princeton, 1960).
[23]M. H. Alexander and S. L. Davis, J. Chem. Phys. **78**, 6754 (1983).
[24]M. H. Alexander, J. Chem. Phys. **71**, 5212 (1979).
[25]C. F. Curtiss, J. Chem. Phys. **49**, 1952 (1969); L. W. Hunter and C. F. Curtiss, *ibid.* **58**, 3824 (1973); L. W. Hunter and R. F. Snider, *ibid.* **63**, 1151 (1974); D. A. Coombe, R. F. Snider, and B. Sanctuary, *ibid.* **63**, 3015 (1975); D. A. Coombe and R. F. Snider, *ibid.* **72**, 2445 (1980).
[26]G. Grawert, Z. Phys. **225**, 283 (1969).
[27]U. Fano and D. Dill, Phys. Rev. A **6**, 185 (1972).
[28]J. Derouard, Chem. Phys. **84**, 181 (1984).
[29]See, for example, the Introduction and the article by S. E. Darden, in *Polarization Phenomena in Nuclear Reactions*, edited by H. H. Barschall and W. Haeberli (University of Wisconsin, Madison, 1971).
[30]See also, J. Derouard, Thesis, University of Grenoble, 1983.
[31]L. Monchick, J. Chem. Phys. **75**, 3377 (1981).
[32]R. N. Dixon and D. Field, Proc. R. Soc. London Ser. A **368**, 99 (1979).
[33]J. Derouard, Abstracts, 10th Colloquium on the Physics of Atomic and Electronic Collisions, Aussois, France, 1984; and to be published.
[34]M. Broyer, G. Gouedard, J. C. Lehmann, and J. Vigué, Adv. At. Mol. Phys. **12**, 165 (1976).
[35]M. D. Rowe and A. J. McCaffery, Chem. Phys. **34**, 81 (1978).
[36]C. E. Gaebe and R. A. Gottscho (unpublished).
[37]J. Derouard and N. Sadeghi (unpublished).
[38]M. H. Alexander and J. Derouard (unpublished).